Effect of the Substituents of the Neighbor Ring in the Conformational Equilibrium of Iduronate in Heparin-like Trisaccharides.

ARTICLE *in* CHEMISTRY - A EUROPEAN JOURNAL · DECEMBER 2012

Impact Factor: 5.73 · DOI: 10.1002/chem.201202770 · Source: PubMed

8 AUTHORS, INCLUDING:

Juan Carlos Muñoz García
University of Oxford
8 PUBLICATIONS **25** CITATIONS
SEE PROFILE

Javier López-Prados
Scientific Research Centre "Isla de la Cartuja"
15 PUBLICATIONS **123** CITATIONS
SEE PROFILE

Jesus Angulo
University of East Anglia
56 PUBLICATIONS **854** CITATIONS
SEE PROFILE

Pedro M Nieto
Spanish National Research Council
96 PUBLICATIONS **2,158** CITATIONS
SEE PROFILE

CHEMISTRY
A EUROPEAN JOURNAL

FULL PAPER

DOI: 10.1002/chem.201202770

Effect of the Substituents of the Neighboring Ring in the Conformational Equilibrium of Iduronate in Heparin-like Trisaccharides

Juan Carlos Muñoz-García,[a] Javier López-Prados,[a] Jesús Angulo,[a] Irene Díaz-Contreras,[a] Niels Reichardt,[b] José L. de Paz,[a] Manuel Martín-Lomas,[b] and Pedro M. Nieto*[a]

Abstract: Based on the structure of the regular heparin, we have prepared a smart library of heparin-like trisaccharides by incorporating some sulfate groups in the sequence α-D-GlcNS-(1-4)-α-L-Ido2S-(1-4)-α-D-GlcN. According to the 3D structure of heparin, which features one helix turn every four residues, this fragment corresponds to the minimum binding motif. We have performed a complete NMR study and found that the trisaccharides have a similar 3D structure to regular heparin itself, but their spectral properties are such that allow to extract very detailed information about distances and coupling constants as they are isotropic molecules. The characteristic conformational equilibrium of the central iduronate ring has been analyzed combining NMR and molecular dynamics and the populations of the conformers of the central iduronate ring have been calculated. We have found that in those compounds lacking the sulfate group at position 6 of the reducing end glucosamine, the population of $^2S_0$ of the central iduronate residue is sensitive to the temperature decreasing to 19 % at 278 K. On the contrary, the trisaccharides with 6-*O*-sulfate in the reducing end glucosamine keep the level of population constant with temperature circa 40 % of $^2S_0$ similar to that observed at room temperature. Another structural feature that has been revealed through this analysis is the larger flexibility of the L-IdoAS-D-GlcN glycosidic linkage, compared with the D-GlcNS-L-IdoA. We propose that this is the point where the heparin chain is bended to form structures far from the regular helix known as kink that have been proposed to play an important role in the specificity of the heparin–protein interaction.

Keywords: carbohydrates · conformation analysis · glycosaminoglycans · molecular dynamics · NMR spectroscopy

Introduction

Heparin and heparan sulfate are glycosaminoglycans (GAG) composed by an uronic acid and a glucosamine 1,4-linked and strongly substituted by sulfate groups that regulate the activity of hundreds of proteins.[1] By means of these interactions the activity of the proteins is regulated and is able to exert a function. The best known example is the interaction with antithrombin, in which a specific and rare sequence of heparin is responsible for the interaction.[2] The interaction occurs in a very selective mode, triggering an enzymatic cascade that results in an anticoagulant activity.[3] Many other proteins require interactions with cell surface glycosaminoglycans (GAGs) to exert their biologic activity.[4] The effect of GAG binding on protein function ranges from essential roles in development, cell growth, cell adhesion, inflammation, tumorigenesis, and interactions with pathogens.[5] Many other examples are not as evident and when the interaction was treated in terms of pharmacophore, it became imprecise and some authors have suggested a continuous range of affinities in function of the substitution pattern or the population of a particular conformation of iduronate, or the presence of a kink in the carbohydrate chain.[6]

From the study of several well-known proteins, it is known that the interactions of heparin or heparan sulfate with proteins, apparently, do not include large conformational changes in the structure of the carbohydrate. Therefore, owing to its nature and topology—a rigid helix with a complete turn every four residues—[7] it can be expected that the interactions with the same side of a protein surface should be discontinued, grouping each three contiguous residues (Figure 1).[1b,8] Additionally, the number and distribution of sulfate groups should play some role in the specificity of the interaction.[9] Another structural key aspect of the heparin or HS structure is that while it is very rigid from the

[a] J. C. Muñoz-García,[+] Dr. J. López-Prados,[+] Dr. J. Angulo, I. Díaz-Contreras, Dr. J. L. d. de Paz, Dr. P. M. Nieto
Glycosystems Laboratory
Instituto de Investigaciones Quimicas, CSIC - US
Americo Vespucio, 49, 41092 Sevilla (Spain)
Fax: (+34) 954-46-01-65

[b] Dr. N. Reichardt, Prof. M. Martín-Lomas
Laboratory of Glyconanotechnology
CIC-BiomaGUNE, CIBER-BBN
Paseo Miramón 182, Parque Tecnológico
20009 San Sebastián (Spain)

[+] These authors have contributed equally to this work

Supporting information for this article is available on the WWW under http://dx.doi.org/10.1002/chem.201202770.

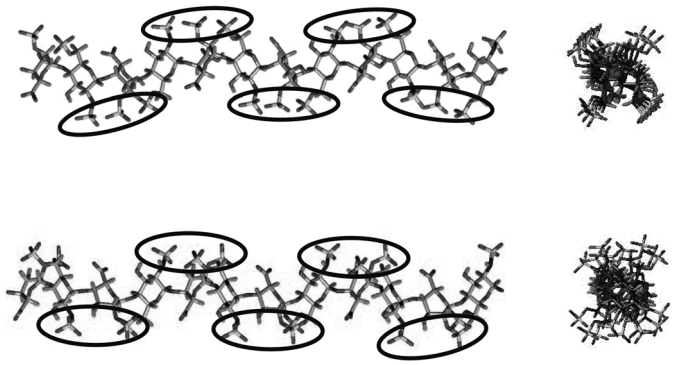

Figure 1. Heparin structures calculated based on NMR restrains of a dodecasaccharide representative of the regular region of heparin with all the iduronates in $^1C_4$ (top) and in $^2S_0$ (bottom). Each group of three contiguous sulfate groups is marked.[7]

backbone perspective, it is also quite flexible when the conformations of iduronate are considered. The internal iduronate residues are in equilibrium between two conformations, the chair $^1C_4$ and the boat $^2S_0$.[7,10] Such equilibrium, however, does not affect to the overall shape of the molecule, which remains linear with the same helical pitch.[8] This is because in spite of the apparent differences between conformations, the relative orientations of the glycosidic bonds linkages are very similar. The final result of the conformational equilibrium correspond to the interchange in the relative positions of carbons C2 and C3 up and down the main plane of the ring, while the atoms in positions C1, O6, C5, and C4 remain in the same relative positions. Thus, when C2 is up the mean plane of the ring and C3 is down the conformation is the chair $^1C_4$ while when the relative positions are the opposite the conformation is the skew boat $^2S_0$.

Based on these premises we have designed and synthesized a small library of eight trisaccharides, **Tri1**–**Tri8** (Figure 2). Assuming that the heparin 3D structure (Figure 1) has a 180° turn every two disaccharides,[7] a trisaccharide GlcN-IdoA-GlcN would cluster three key sulfate groups toward the same side of the molecule originating a minimum recognition site,[11] while a potential adjacent second site is necessarily directed towards the opposite direction, in an antiparallel orientation, or shifted by two residues in a parallel fashion (Figure 3). Therefore the complementary trisaccharide IdoA-GlcN-IdoA should not be able to interact with a single binding site within the protein, but could establish a bridge between two receptors, as frequently found by X-ray crystallography. Starting from the basic trisaccharide D-GlcN2S-L-IdoA2S-D-GlcN, and assuming that the two sulfate groups are driving the main interaction, we have permutated the rest of the potential sulfation sites except the position 3 of glucosamine that has only been reported in the interaction with antithrombin.[12] We have replaced the sulfate groups by an uncharged substituent present in the general structure of heparin of heparan sulfate. Thus, the N sulfamate in position 2 was substituted by an N-acetamido group as it is more frequent in heparin than the amino group, additionally it does not change the overall charge of the system, while the sulfate in position 6 of glucosamine was not replaced, thus leaving an hydroxyl group. We have decided not to permutate the carboxylate group of the iduronate because this replacement has not been reported in the regular region of heparin and it is a key element in the control of the conformational equilibrium of the iduronate ring.

Herein we describe the synthesis, NMR analysis, and the MD simulations of the library of trisaccharides. We have found some interesting effects of the temperature on the equilibrium of the central iduronate residue, as well as selec-

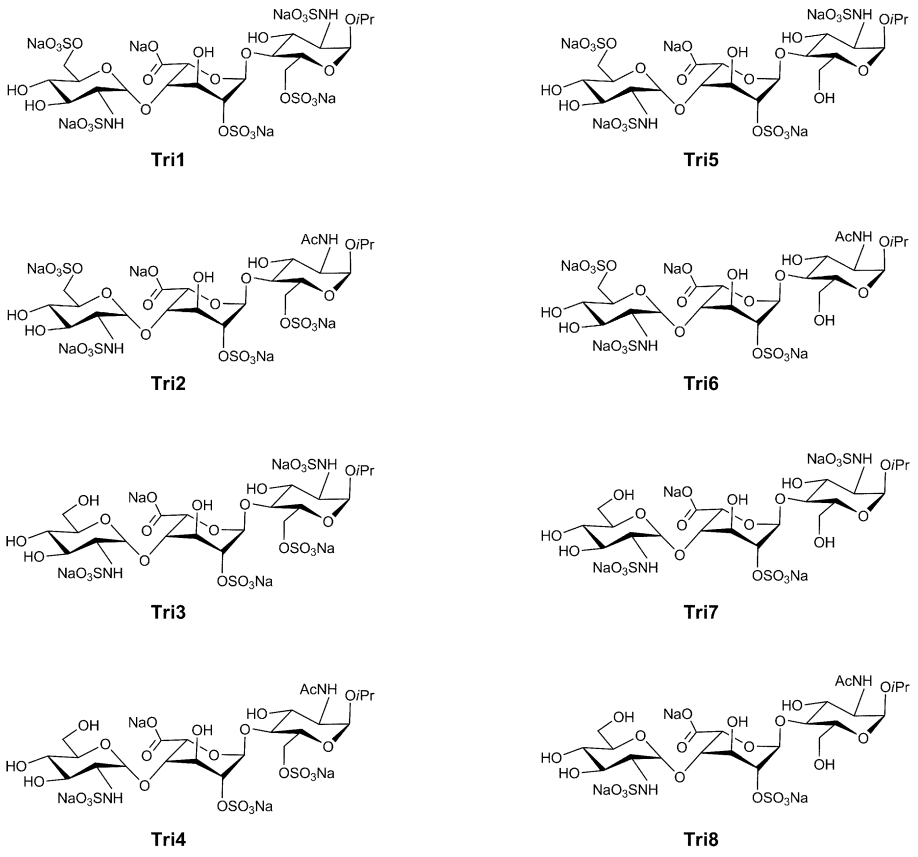

Figure 2. Library of heparin trisaccharides drawn displaying the 3D relative disposition up or down of the substituents. Nomenclature A, B, C is used for definition of the rings throughout the text.

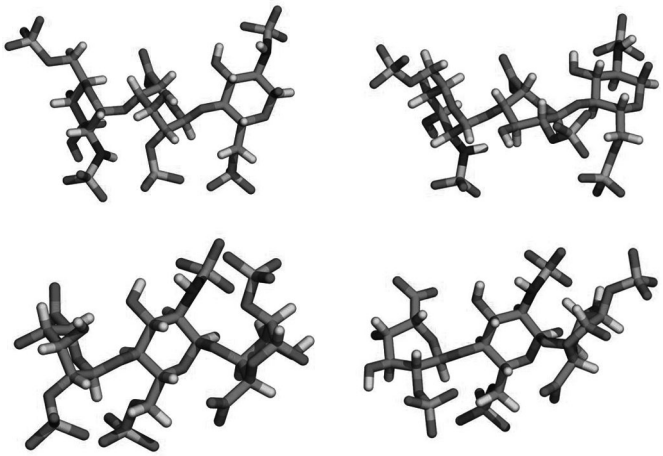

Figure 3. Trisaccharide **Tri1** in $^1C_4$ chair conformation (up left) and in $^2S_0$ skew boat conformation (up right), and complementary trisaccharide in $^1C_4$ (down left) and in $^2S_0$ (down right).

tive hydration shell depending on the conformation of such residue.

Results

Synthesis of a library of heparin-like trisaccharides: We carried out the synthesis of the trisaccharide library following the retrosynthetic analysis shown in Scheme 1. Monosaccharide building blocks **1–4** were glycosylated with disaccharide donor **5**[13] to obtain the fully protected intermediates required for the synthesis of the final sulphated trisaccharides.

Building blocks **1** and **2** containing a 2-acetamido functionality were prepared from *N*-acetyl-D-glucosamine (Scheme 2). Fischer glycosylation with isopropyl alcohol followed by benzylidenation afforded **6** in good yield. Benzylation of the 3-hydroxyl group gave **7**, which was then submitted to reductive benzylideneacetal opening with $NaCNBH_3$ and HCl[14] to obtain building block **1**. Alternatively, hydrolysis of the benzylideneacetal in **7**, and then selective 6-OH benzoylation gave building block **2**.

The synthesis of the two monosaccharidic building blocks containing a 2-azido functional group, **3** and **4**, started with the glycosylation of the known trichloroacetimidate **8**[15] with isopropanol under standard conditions (Scheme 3). Further transformation of the benzylideneacetal moiety in **9** as described above yielded the desired building blocks **3** and **4**.

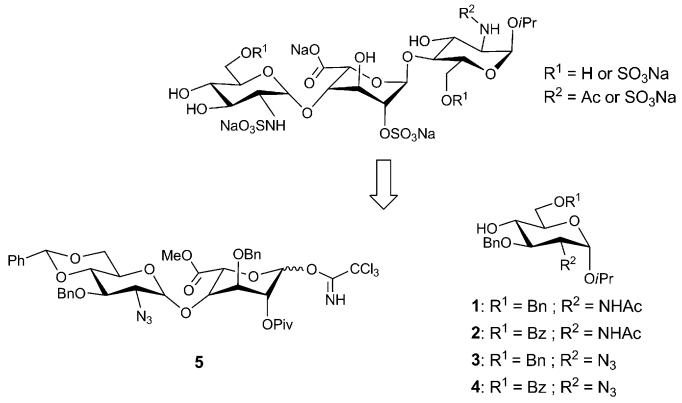

Scheme 1. Retrosynthetic analysis.

Trisaccharides **10**, **11**,[16] **12**, and **13** were obtained in good yield by glycosylation of the monosaccharide building blocks **1–4** with the known disaccharide trichloroacetimidate **5** (Scheme 4). These fully protected intermediates were submitted to the deprotection/sulfation reaction sequence to give the four heparin trisaccharides that do not contain a sulfate group at position 6 of the non-reducing end.

The removal of methoxycarbonyl and acyl groups was performed with lithium hydroperoxide and then aqueous/alcoholic potassium hydroxide to minimize the β-elimination of iduronic ester.[17] The resulting partially protected trisaccharides **14–17** were O-sulfated by treatment with fresh SO_3•Me_3N complex in dimethylformamide (DMF) at 50 °C. Staudinger reduction of the azide protecting groups in **18–21** with Me_3P and NaOH, followed by N-sulfation with fresh SO_3•Py complex afforded trisaccharides **22–25** in excellent yield.[18] Reverse phase C-18 chromatography, using an aqueous Et_3NHOAc buffer (10 mM) at pH 7 as mobile phase with a MeOH gradient,[19] was required to obtain high purity

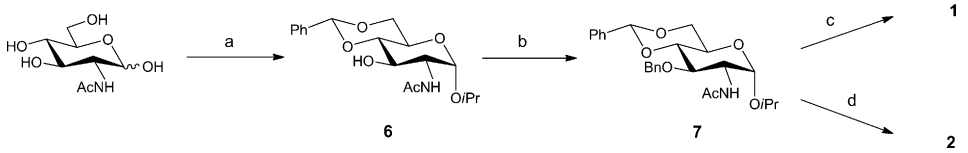

Scheme 2. Synthesis of building blocks **1** and **2**. a) i) Amberlite IR-120, *i*PrOH, 70 °C, 48 h, ii) benzaldehyde dimethyl acetal, *p*TsOH (cat.), DMF, 50 °C, 2 h, 77 %. b) BnBr, TBAI, NaH, CH_2Cl_2, RT, 24 h, 86 %. c) $NaCNBH_3$, HCl, THF, 4 Å M.S., RT, 10 min, 90 %. d) i) TFA, H_2O, CH_2Cl_2, 1 h, RT, ii) BzCl, Et_3N, CH_3CN, −30 °C, 2 h, 86 %.

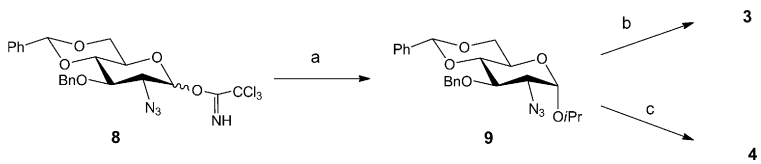

Scheme 3. Synthesis of building blocks **3** and **4**. a) *i*PrOH, TMSOTf, CH_2Cl_2, 0 °C, 30 min, 70 %. b) $NaCNBH_3$, HCl, 4 Å M.S., THF, RT, 15 min, 92 %. c) i) TFA, H_2O, CH_2Cl_2, RT, 30 min, ii) BzCl, Et_3N, CH_3CN, −30 °C, 2 h, 86 %.

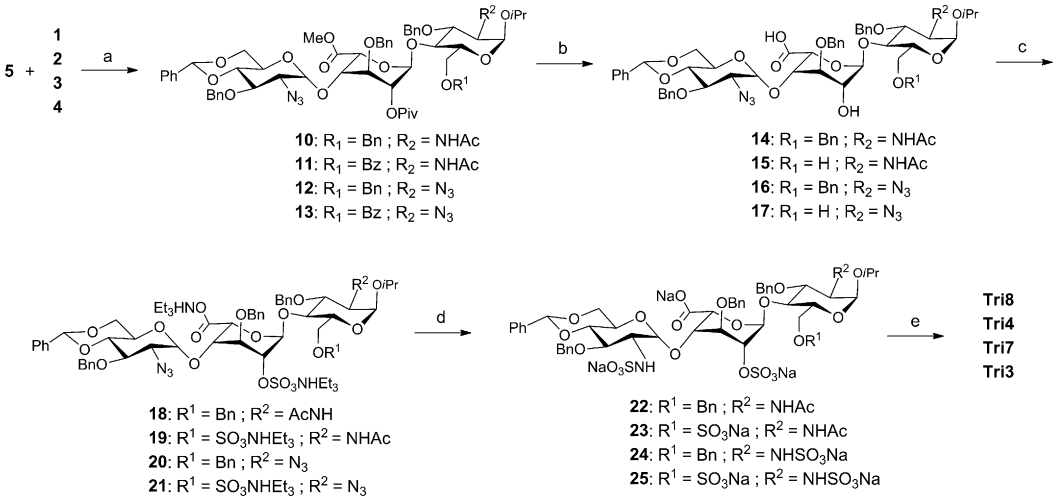

Scheme 4. Synthesis of trisaccharides **Tri3**, **Tri7**, **Tri4**, and **Tri8**. a) TMSOTf, CH_2Cl_2, 4 Å M.S., RT, 1 h, 75–91%. b) i) 30% H_2O_2, 1 N LiOH, THF, RT, 1 day, ii) 3 N KOH, MeOH, RT, 1 day, 87–92%. c) SO_3•Me_3N, DMF, 50°C, 24–72 h, 78–92%. d) i) 0.1 N NaOH, Me_3P, THF, RT, 1–4 h, ii) SO_3•Py, Py/Et_3N = 5:1, RT, 30 min, 81–94%. e) H_2, $Pd(OH)_2$/C, MeOH/H_2O = 9:1, RT, 92–96%.

O- and N-sulfated products. Finally, global deprotection with $Pd(OH)_2$/C led to the desired trisaccharides**Tri8**, **Tri4**, **Tri7**, and **Tri3**.

For the synthesis of the trisaccharides with a sulphate group at the 6 position of the non-reducing end glucosamine unit, trisaccharides **10–13** were first submitted to the reductive opening of the benzylideneacetal (Scheme 5). Et_3SiH was used as the reductive reagent and dichlorophenylborane as the acid,[20] obtaining the corresponding 4-*O*-benzyl-6-hydroxy derivatives **26–29** in optimal yield with excellent selectivity. These derivatives were then subjected to the deprotection/sulfation sequence as described above to give trisaccharides **Tri6, Tri2, Tri5**, and **Tri1**.

Interestingly, we found that the O sulfation of **31** using SO_3•Py complex in pyridine as solvent gave a mixture[21] of the desired product **35a** in 45% yield and the lactone[22] **35b** in 52% yield, while the use of SO_3•Me_3N complex in DMF at 50°C gave **35a** in excellent 91% yield without detection of the lactone side product (Scheme 6).

Nuclear magnetic resonance: All the compounds have been ^1H and ^{13}C assigned at several temperatures (see the Supporting Information). First, the spins systems resonances from the three hexoses and the isopropyl group were assigned using COSY and TOCSY, thus obtaining spin systems that were connected by interglycosidic NOE or ROE contacts between the anomeric proton and H4 or H3 and H4,

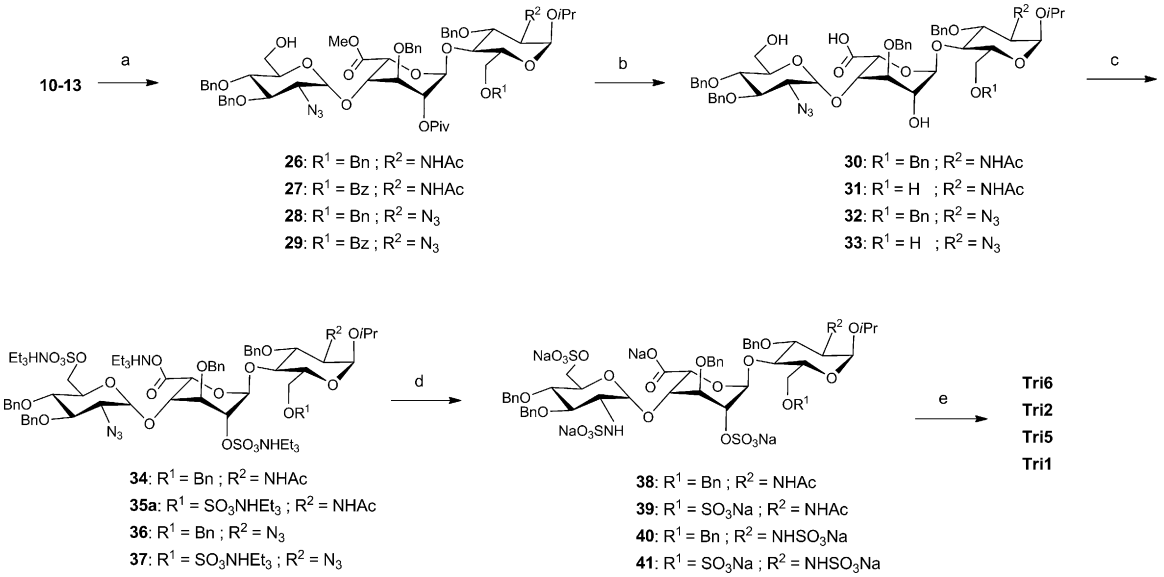

Scheme 5. Synthesis of trisaccharides **Tri6**, **Tri2**, **Tri5**, and **Tri1** a) Et_3SiH, dichlorophenylborane, CH_2Cl_2, −78°C (5 min)→−40°C (30 min), 84–91%. b) i) 30% H_2O_2, LiOH, THF, RT, 1–2 days, ii) 3 N KOH, MeOH, RT, 1–5 days, 72–91%. c) SO_3•Me_3N, DMF, 50°C, 1–5 days, 88–92%. d) i) 0.1 N NaOH, Me_3P, THF, RT, 1–2 h, ii) SO_3•Py, Py/Et_3N = 5:1, RT, 30–60 min, 85–89%. e) H_2, $Pd(OH)_2$/C, MeOH/H_2O = 9:1, RT, 95–97%.

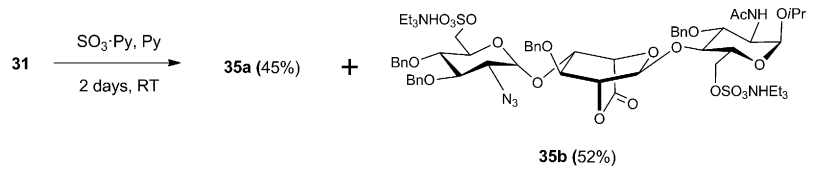

Scheme 6. Detection of a lactone side product in the O-sulfation of intermediate **31**.

thus corresponding to a preferentially *syn* rearrangement of the glycosidic linkage.[7] The effects of sulfonation on the ^{1}H and ^{13}C chemical shifts correspond to the effects described, observing a downfield shift of both the ^{1}H adjacent and the ^{13}C ipso (see the supporting information).[23] The larger downfield effects are observed in positions 2 and 6 of ring A and 6 of ring C. Interestingly, the H6 protons on ring A are isochronous while those of ring C have different chemical shift being the differences larger for the 6-*O*-sulfoderivatives. When the different compounds were compared, all the L-IdoA2S resonances were well clustered except those for H5 that were dispersed without any apparent reason.

NOESY, ROESY, and 1D-NOESY, 1D-ROESY, and 1D-T-ROESY experiments have been performed to build the growth curves in order to quantify the experimental distances based on sigma NOE or sigma ROE.[24] The results at room temperature are consistent with a molecule in a motion regime close to the NOE zero-crossing point, thus implying low intensities and difficulties to integrate because of the low accuracy. At the same temperature ROE peaks, although measurable, were too influenced for undesired effects of strong coupling and other artifacts. TOCSY transfer of magnetization was frequently detected; in particular the more interesting ones that correspond to the iduronate ring as result of their minor chemical shift dispersion. Attempts to solve the problem using 1D-T-ROESY did not give better results. We decided to vary the temperature in order to modify the correlation time, and the best results were obtained at low temperatures (278–283 K) using 1D-NOESY.[25] At high temperatures (308–313) the zero crossing was still a problem in some cases. Because of the comparative nature of this work we decided to use low temperature in this study as it allowed us to analyze all the compounds in the same conditions. Based on the 2D-NOESY spectra we constructed the growing-up NOE curves for those protons of particular interest via mono dimensional selective analogues of NOESY (dpfgse-NOESY) as they have a larger linearity and better quality than the 2D analogues[26] (Figure 4). Using the isolated spin-pair approximation[27] we have calculated the interprotonic distances by the ratio of their respective sigma NOE (see below) obtained by two independent methods: either fitting the whole curve to a biexponential equation or to a linear growth using a relative distance (see Table 1 and the Supporting Information).

At low temperatures, the interglycosidic NOEs are indicating a *syn* rearrangement of the glycosidic linkages. However, at high temperature (298 K) other minor NOE cross-peaks (H1′–H5, H1′–H3, and H2′–H5) corresponding to an *anti* arrangement for the first glycosidic linkage can be observed together with a larger NOE (H1′–H4), exclusive of the *syn* conformation (Figure 5).

Regarding the conformation of the iduronate ring, the analysis of the coupling constant and the observation of the exclusive H2′–H5′ contact (NOE, ROE, T-ROE) indicate a contribution of the $^{2}S_{0}$ conformer in equilibrium with the $^{1}C_{4}$ chair. (Figure 5 and Figure 6). This is a characteristic feature

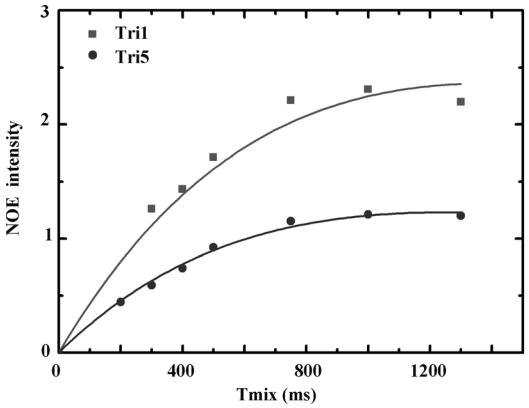

Figure 4. 1D-NOESY growth curves (at 278 K) corresponding to the H2–H5 distance of trisaccharides **Tri1** ($6OSO_3^-$ reducing end) and **Tri5** (6OH reducing end).

Table 1. Experimental and theoretical interglycosidic key distances. The theoretical values were averaged over 40000 frames of MD simulation and weighted on the populations of chair $^{1}C_{4}$ and skew boat $^{2}S_{0}$ conformations at 278 K. The theoretical H1′–H6 distances represent the r-6 average over the *pro R* and *pro S* values. Linear regression was used to calculate the experimental distances.

	Method	Distance [Å]						
		GlcN-IdoA2S		L-IdoA2S	IdoA2S-GlcN			
		H1″–H3′	H1″–H4′	H1′–H3′	H2′–H5′	H1′–H3	H1′–H4	H1′–H6
Tri1	MD	2.3	2.8	3.6	3.2	3.1	2.5	3.5
	exptl	2.6	2.7	3.0	3.0	–	2.5	–
Tri2	MD	2.3	2.9	3.6	3.1	2.9	2.4	3.4
	exptl	2.6	2.6	3.0	2.9	–	2.4	–
Tri3	MD	2.3	2.8	3.6	3.2	3.9	2.3	3.4
	exptl	2.6	2.7	3.0	2.9	–	2.6	–
Tri4	MD	2.3	2.8	3.6	3.2	3.8	2.3	3.2
	exptl	2.7	2.7	3.0	2.9	–	2.5	–
Tri5	MD	2.3	2.8	3.9	3.5	3.8	2.3	3.6
	exptl	2.6	2.6	–	3.2	–	2.6	–
Tri6	MD	2.3	2.6	3.9	3.5	3.4	2.4	3.5
	exptl	2.6	2.6	3.2	3.2	–	2.6	–
Tri7	MD	2.3	2.7	3.9	3.5	3.7	2.3	3.4
	exptl	2.6	2.6	3.2	3.2	–	2.5	-
Tri8	MD	2.3	2.8	3.8	3.3	3.9	2.3	3.3
	exptl	2.6	2.6	3.1	3.0	–	2.6	–

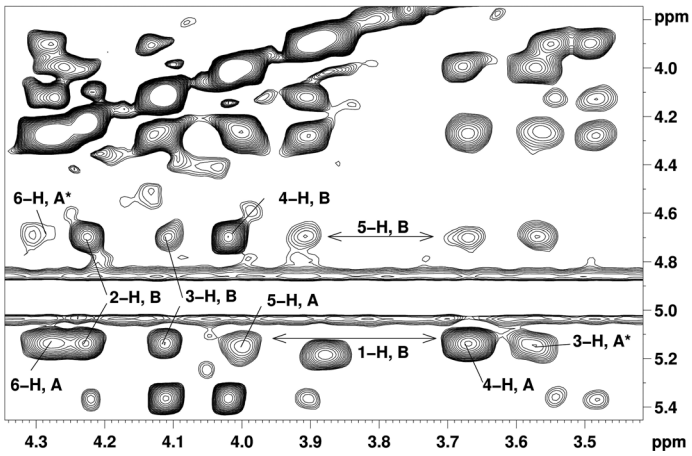

Figure 5. Expansion of a NOESY experiment for **Tri1** showing the signals corresponding to an *anti* rearrangement together with the *syn* rearrangement. Note that latter has the biggest intensity. Exclusive NOE peaks of the *anti*-Ψ conformation are marked with a star symbol.

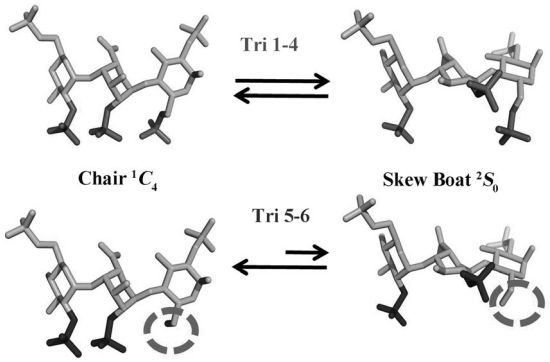

Figure 6. Iduronate conformational equilibrium between $^1C_4$ and $^2S_0$.

of the internal iduronate ring in heparins and heparin-derived oligosaccharides. In this case, we have been able to measure with high precision the coupling constants as to allow us to derive populations (See the Supporting Information and the Molecular Dynamics section).[38,28] We have observed a larger contribution of $^1C_4$ for the compounds without sulfate in position 6 of the reducing end glucosamine, **Tri5**, **Tri6**, **Tri7**, **Tri8**, than for those with sulfate which is reflected in a longer H2′–H5′ distance (3.0–3.2 Å; Table 1) than the sulfated ones (2.9–3.0 Å; Table 1). In addition, we have found differences in temperature dependence for those lacking of sulfate into position 6 of reducing end glucosamine. This behavior is consistent with a decrease of the $^2S_0$ population from 40% to 35%–25%, when the temperature is decreasing from 323 to 283 K. Interestingly, in trisaccharides bearing sulfates on position 6 of reducing end glucosamine this dependence is not observed and the skew boat population remains constant above 40% along all the range of temperatures.

Molecular dynamics (MD): The iduronate ring exhibits a characteristic conformational equilibrium, that for inner residues involve two conformations, $^1C_4$ and $^2S_0$. Thus, as the characteristic interconversion rate within the millisecond time scale is far from the MD accessible range, two alternative approaches can be used: first consider two different starting geometries for the iduronate residues and run two independent molecular dynamic simulations, and second use experimental restrictions and run a single time averaged restrained molecular dynamic simulation. In this work we have used the first approach and two alternative starting conformations for the iduronate ring were considered to account for the conformational equilibrium: $^1C_4$ and $^2S_0$. The global results were thus obtained by weighting both simulations according to their respective populations calculated from the experimental results about the conformational equilibrium obtained from coupling constant analysis.[28]

Global geometry: analysis of interglycosidic torsions: First, to define the global geometries of trisaccharides, we analyzed the dynamic behavior of the two glycosidic linkages of each trisaccharide by monitoring the torsions Φ (H1′-C1′-O-C4) and Ψ (C1′-O-C4-H4) along the molecular dynamics simulation. Qualitatively the effect of the conformational change between $^1C_4$ and $^2S_0$ conformations is subtler than it can be expected, affecting only to the relative position of the carbons C2 and C3 of the iduronate ring, while the relative positions of the C1, C4, C5, and O6 remained the same. Therefore for the change between both conformations only the relative positions of C2 and C3 must be swapped.

In the case of the GlcN-IdoA linkages, the simulations predict interglycosidic distances H1″–H4′ and H1″–H3′ within the range for NOE observation, in good agreement with the experimental NMR data (Table 1). In general, the distributions of Φ and Ψ were centered at −60° and −50°, respectively (see the Supporting Information). The distributions in the case of $^2S_0$ conformation were narrower and in the case of the $^1C_4$ the data predict an increase in the local flexibility of the GlcN-IdoA glycosidic linkage, principally in the Φ angle although correlated with a minor effect in the Ψ torsion (see the Supporting Information).

A parallel analysis for the IdoA-GlcN linkages reveals that when the L-IdoA residues were in the $^1C_4$ conformation, the Φ torsion was distributed between 0° and 60°, with a maximum close to 60°, whereas in the case of the $^2S_0$ conformation, this interval was somewhat modified (from 0° to 75°), slightly increasing the accessible conformational space. The Ψ torsion was significantly more flexible and showed a behavior sensitive to the conformational state of the L-IdoA ring. In particular, for the $^2S_0$ conformation of the central ring some population of *anti*-Ψ conformers ($\Psi = \pm 180°$), over 30%, were predicted for three (**Tri1**, **Tri5**, and **Tri6**) out of the eight trisaccharides (see the Supporting Information), as well as significant differences in the relative populations of conformers at the two sub-minima (centered at −60° and 0°) for different trisaccharides. Yet, these differences could not be easily correlated to the sulfation pattern. In the NMR spectroscopic study, the *anti*-Ψ conformation was detected in some favorable cases (observation of the set of

NOEs H1′–H3, H5′–H6a, and H5′–H6b; see Figure 5). The simulations predicted interglycosidic distances H1′–H4, H1′–H3, and H1′–H6 (*pro R* or *pro S*) within the range for NOE observation, once more in agreement with the experimental NMR data (Table 1).

A description of the global geometries of the trisaccharides in solution must also take into account the different populations of conformers of the central L-iduronate ring. As the timescale for ring interconversion is out of the feasible current molecular dynamics capabilities (above microseconds), we have included this effect by using the populations experimentally obtained, as described below (Figure 7). With these data, we have weighted the ensembles of Φ and Ψ values by the populations of $^1C_4$ and $^2S_0$ conformers at 298 K (Figure 7). The results indicated that for

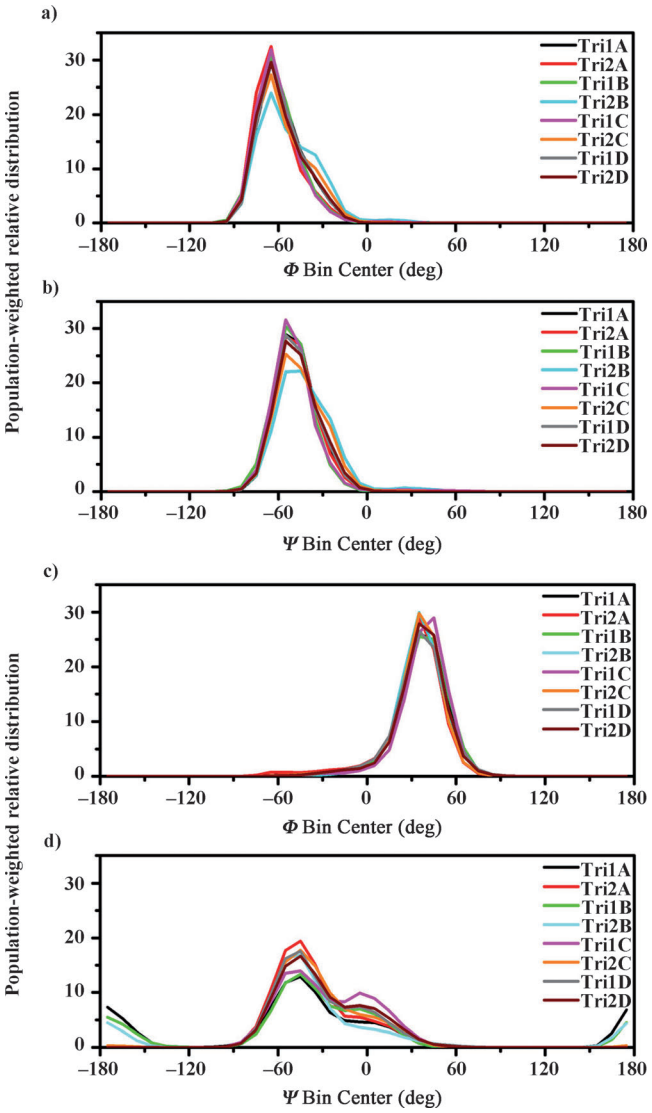

Figure 7. Population-weighted distribution curves for the glycosidic torsions Φ and Ψ of the glycosidic linkages a, b) GlcN-IdoA2S and c, d) IdoA2S-GlcN for the whole library of trisaccharides. The populations of conformers at 298 K have been taken for the weighting. A bin size of 30° has been used.

GlcN-IdoA linkages, the weighted distributions of Φ and Ψ were centered at −65° and −50°, respectively (Figure 7). Both torsions were quite rigid and there was no apparent influence of the sulfation pattern. For IdoA-GlcN linkages, the weighted distributions were centered at 40° for the Φ torsion, and 0° and −45° (two subminima) for the Ψ torsion. Some minor contribution from *anti*-Ψ conformers was observed when the central IdoA residue was in $^2S_0$ conformation. As before, the sulfate pattern did not seem to impose any noticeable effect on the IdoA-GlcN conformational space (Figure 7).

Solvation and hydrogen bonds: The analysis of the radial distribution functions (rdf) identified a generalized effect of the L-IdoA2S conformation on the solvation around the glycosidic oxygen atoms of the IdoA2S-GlcN linkages (see the Supporting Information). Specifically, when the L-IdoA2S residue adopts the $^2S_0$ conformation, two solvation shells at 2 and 3 Å appear around this glycosidic oxygen, which are absent in the $^1C_4$ conformation. Thus, these two solvation shells are skew boat $^2S_0$ exclusive. This observation is interesting in the context of L-IdoA2S interactions with proteins, as it indicates that the structuration of the molecular solvation shell is sensitive to the conformational state of the iduronate ring.

We also analyzed the presence of inter-residual hydrogen bonds. For that purpose we have chosen a distance and angle cutoff of 3.0 Å and 120°, respectively (see the Experimental Section). The results allowed us to identify a conserved hydrogen bond involving the oxygen ring of the L-IdoA2S residue and the hydrogen H3O of the reducing end GlcN (see Figure 19S in the Supporting Information). It appears with an average occupancy of 57%, an average lifetime of 2.6 ps, an average distance of 2.4 Å, and an average angle of 32°. Furthermore, it is not influenced by the conformation of the L-IdoA2S residue or the sulfation pattern. Other conserved hydrogen bond found was that between oxygen O5 of the non-reducing end GlcN and the hydrogen H3O of the L-IdoA2S residue. Nevertheless, this hydrogen bond presented a low average lifetime (below 1 ps) and a low percentage of occupancy (below 20%; see the Supporting Information).

Populations of central iduronate conformers: We have monitored the four inter-proton dihedral angles (H1′-C1′-C2′-H2′, H2′-C2′-C3′-H3′, H3′-C3′-C4′-H4′, H4′-C4′-C5′-H5′) of the L-IdoA2S residue for both $^1C_4$ and $^2S_0$ starting conformations along the 40000 frames of each trajectory obtained. From these values (see the supporting information), vicinal proton–proton coupling constants, $^3J_{HH}$, for each frame and conformation have been calculated by using the Haasnoot–Altona equation, which takes into account both the electronegativity and the orientation of the substituents on the fragment H-C-C-H.

The final theoretical $^3J_{HH}$ values for $^1C_4$ and $^2S_0$ have been obtained as an average for each of the models (L-IdoA2S in $^1C_4$ or in $^2S_0$) from the torsional angles calculated from the

frames obtained along the trajectories. Next, to obtain the populations of conformers ($^1C_4$ and $^2S_0$) of the L-IdoA ring in each trisaccharide, we carried out an iterative fitting of theoretical and experimental *J*-coupling data [Eq. (1)]. At this point the $^4C_1$ conformation was disregarded as no experimental support was obtained for it, particularly the exclusive GlcN-IdoA H5′-H5 NOE was not observed.[29]

Therefore, the experimental $^3J_{HH}$ coupling constants were considered as averages of the MD-derived $^3J_{HH}$ for each conformer weighted on the molar fraction of each one.[28] As the theoretical values were averages from MD simulations, they implicitly reflected the fluctuations around canonical conformations, which must be considered for this flexible hexopyranose ring[28] particularly to account for the pseudorotational conformational space in the case of the skew boat conformer ($^2S_0$).

The results are shown in Figure 8, classified by the two series of trisaccharides. Those with a sulfate group in position 6 of the glucosamine at the reducing terminal **Tri1**, **Tri2**,

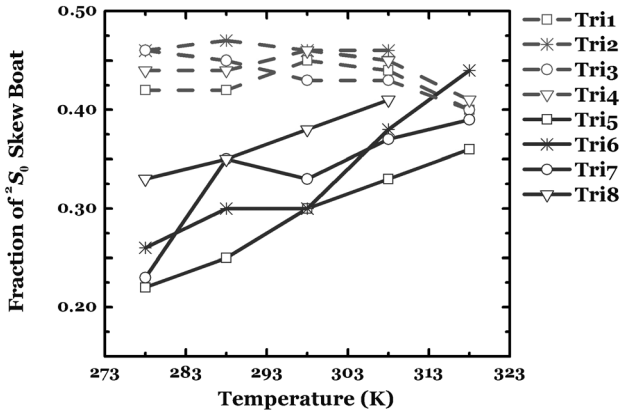

Figure 8. Variation of $^2S_0$ conformer population as a function of the temperature. Two different behaviors depending on the substitution on position 6 at the reducing end glucosamine (Glc-A) are observed.

Tri3, and **Tri4** (dotted lines) and those lacking this group **Tri5**, **Tri6**, **Tri7**, and **Tri8** (full lines). The data revealed clear differences between both series in the behavior of the conformer populations of the L-IdoA2S ring as a function of temperature. Explicitly, we have observed conformational differences (Figure 8) that were specific to the presence or absence of the 6-*O*-sulfate group on the reducing GlcN ring. Particularly, the absence of this bulky charged group made the $^2S_0$ population very sensitive to temperature (Figure 8). At low temperature (278 K) the $^1C_4$ conformer was favored in second ensemble (65–80%), while it remained basically unchanged in the first one (53–57%). As the temperature increased, the differences between both ensembles started to vanish.

The combination of NMR spectroscopy and MD simulations (Figure 8) demonstrate a significant influence of the sulfation pattern on the conformational equilibrium of an internal L-IdoA2S residue. As one major energy component in protein–heparin interactions is the electrostatic term, it is tempting to speculate on the importance of the electrostatic compensation of ligand "internal energy stresses" (as those present in the triad of sulfate groups) by the positively charged sidechains of amino acid typically found in the binding sites of heparin-binding proteins, on the modulation of the L-iduronate conformations in the bound state.

Correlation times: Finally, we have performed the analysis of the global time correlation function from the molecular dynamics data. Overall correlation times (τ_0) for the eight trisaccharides were calculated according to the model-free approach[30] by first calculating the auto correlation function for each H–H vector with AMBER, and considering the conformational equilibrium and the conformers populations. The results (see Figure 9) show a very significant increase in

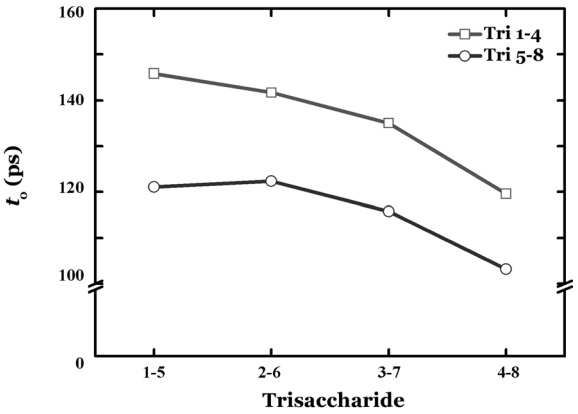

Figure 9. Global time correlation (τ_0) at 298 K of each trisaccharide weighted in populations determined by $^3J_{HH}$ analysis.

the global time correlation for the ensemble of trisaccharides with sulfate groups in the position 6-*O* of the reducing end glucosamine compared with those with a hydroxyl group in that position. This is evident when compare the pair **Tri3** and **Tri5**, which have the same formula differing in the position of the 6-*O*-sulfate group. Thus, the removal of the 6-*O*-sulfate group on the reducing GlcN ring gives rise to the reduction in the global time correlation, and therefore, a faster reorientation in solution for the trisaccharides belonging to this ensemble.

Discussion

For the synthesis of the eight heparin-like trisaccharides, we have followed a 2+1 glycosylation approach that used disaccharide **5** and monosaccharides **1–4** as key building blocks. We have employed an appropriate set of protecting groups to obtain the required stereochemistry of the glycosidic linkages and introduce the sulfate groups at the desired positions. This strategy has allowed the preparation of the trisaccharides in good overall yield.

The minimum size of these trisaccharides, lead to the absence of a preferential axis of rotation and the molecules behave as spherical particles in isotropic motion, allowing us to quantify the distances from NOESY build up curves by assuming an isotropic behavior. In case of larger glycosaminoglycans, longer than 5–6 residues, the rigidity of the glycosidic linkage causes a top rotor behavior featuring two perpendicular axis of rotation with two different correlation times[31] and as a consequence of the effect of the anisotropy a more complex and inaccurate method of distance evaluation is needed as the intensity of the NOE depends not only on the distance but also on the angle between the interprotonic distance and the axis of the molecule.[32] Therefore, the distances obtained from the analysis of NOESY cross-peaks in from trisaccharides should be more accurate in our library than those obtained from larger compounds.

The smaller size also affords narrower signals, allowing the extraction of reliable coupling constants, and therefore to analyze more accurately the conformational equilibrium of the central L-Ido2S ring, which is in equilibrium between the $^1C_4$ and $^2S_0$ conformations. This is a characteristic feature of the internal iduronate residues in heparin, and has been thoughtfully studied.[33] Chemical purity of these synthetic molecules and their designed patterns of substitutions make this set of eight trisaccharides an excellent framework to study the effect of differences in sulfation on the conformational behavior of the L-Ido2S rings. As this ring holds a sulfate group at position 2 in all the trisaccharides, we are exclusively analyzing the effects of sulfation of adjacent residues on the conformation of the central L-iduronate 2-O-sulfate.

From the experimental determination of proton–proton distances (Table 1) we firstly focused our analysis on those defining the local conformation of the L-IdoA2S residue. The observation of a NOE signal between protons H2′–H5′ reveals the presence of the conformation $^2S_0$, however, from the analysis of coupling constants is clearly deduced the participation of other conformations, particularly $^1C_4$. The detailed analysis of the distances H1′–H2′, H1′–H3′, H2′–H5′ and H4′–H5′ for L-IdoA2S residue shed light on its conformation. Thus, the calculated values for the H4′–H5′ distance (between 2.4 and 2.6 Å) are in agreement with a equilibrium between the canonical $^1C_4$ and $^2S_0$ conformations. Furthermore, the absence of H5″–H5′ NOE cross-peak for the GlcN-IdoA2S glycosidic linkage confirmed that the chair $^4C_1$ conformation for the L-IdoA2S residue is not present in solution. Regarding the H1′–H2′ distance, the results show consistently shorter values in the trisaccharides without sulfate group in position 6 of the reducing end glucosamine, compounds **Tri1**–**4**. Since this distance (according to the canonical conformations) is longer in the $^2S_0$ conformer, this observation agrees with a higher $^2S_0$ population in the **Tri1**–**4** ensemble (see Table 1). The H1′–H3′ and H2′–H5′ NOESY signals, which correspond to exclusive NOEs of the $^2S_0$ conformation of the L-IdoA2S residue, are also clearly observed. Thus, the results confirm the presence of the $^2S_0$ conformer in the whole library of trisaccharides. Moreover, the shorter values obtained for both distances in the **Tri1**–**4** ensemble demonstrate the existence of a higher population of the $^2S_0$ conformer in solution when the 6-OSO_3 group is present in the reducing end GlcN residue.

However, the most interesting feature of this conformational equilibrium is the influence of the temperature and substitution pattern. The trisaccharides lacking the sulfate group in position 6 of the reducing end glucosamine (**Tri5**–**Tri8**) have proportions of $^2S_0$ skew boat smaller that decrease with temperature down to 19–28 % at 283 K (see Figure 8). On the contrary, the trisaccharides having a sulfate in the primary position (**Tri1**–**Tri4**) did not show any influence of temperature from 283 to 313 K in the conformational equilibrium with a constant population of $^2S_0$ of 40 %. Considering that the main effect caused by the change from $^1C_4$ to $^2S_0$ is the exchange between the relative positions up and down the mean plane of the ring of carbons 2 and 3, a possible explanation for this behavior could be the electrostatic repulsion between the charges of sulfate in position 2 of L-Ido2S and the adjacent glucosamines (the sulfate in position 6 of glucosamine of the reducing end and the N-sulfate of glucosamine at the other end). The three groups form a cluster of charges that in the case of the compounds with sulfate in the position 6 of the reducing end the only possibility to release the electrostatic energy is to slide to the $^2S_0$ conformation were the charges are further dispersed. On the contrary, in the case of the trisaccharides without this charge where there are only two charged groups in that side of the molecule, the electrostatic interactions may be relieved by rotating the sulfate group to a more favorable position.

Considering now the global conformation, this is going to be directed by the glycosidic linkages, the interglycosidic distances defining the GlcNS-IdoA2S linkage (H1″–H3′ and H1″–H4′) are very similar for all the trisaccharides (from 2.6 Å to 2.7 Å), showing a more rigid behavior for this linkage. This observation is in good agreement with the results obtained from the MDs. Finally, referring to the L-IdoA2S-GlcN glycosidic linkage, due to overlapping we have only been able to quantify the H1′–H4 distance which ranks from 2.4 to 2.6 Å. However, does not show correlatable differences with any structural feature. Furthermore, we have identified NOE peaks corresponding to the H3 and both H6 protons of the reducing end glucosamine from the anomeric position. However, in four of the eight trisaccharides (**Tri1**, **Tri3**, **Tri5**, **Tri7**) the observation of the NOE intensity for the H3 proton could belong to either a inter-glycosidic H1′–H3 short distance or an intra-residue (IdoA2S) H1′–H3′ distance, thus not being able to confirm its existence. In any case, of the trisaccharides **Tri2**, **Tri4**, **Tri6**, and **Tri8**, both H1′–H3 and H5′–H6 NOE signals have been clearly identified (from weak to medium intensities, but are not quantifiable due to overlapping). The simultaneous presence of both NOE intensities confirms the existence of *anti-*Ψ conformer population for the L-IdoA2S-GlcN glycosidic linkage, indicating a larger flexibility of this terminal linkage as compared with α-D-GlcN-(1-4)-α-L-IdoA.

Conclusion

In summary, the study of the influence of the sulfation pattern on the conformational equilibrium of an internal L-IdoA2S has allowed us to confirm that the presence of 6-*O*-sulfation on the reducing end GlcN pushes the equilibrium of the L-IdoA2S ring towards the skew boat $^2S_0$ conformation. This result, which has never been reported so far, is very important because it demonstrates that the substitution of charged functional groups on heparin-like oligosaccharides does not only alter its interaction energy with a protein receptor (absence or presence of key functional groups), but it can also cause a deep effect on the intrinsic conformational properties.

Related to the latter, the trisaccharides lacking the sulfate group in position 6 of the reducing end glucosamine (**Tri5**–**Tri8**) present a temperature-sensitive population of $^2S_0$ skew boat conformers, which decreases from 313 to 283 K. On the contrary, the conformational equilibrium of trisaccharides presenting a sulfate group in the primary position (**Tri1**–**Tri4**) did not show any influence with temperature (range 283–313 K). Thus, we have hypothesized that the electrostatic repulsion between the charges of the sulfate group in position 2 of L-IdoA2S residue and the adjacent sulfates groups of both glucosamines residues forces the L-IdoA2S ring to slide to a skew boat $^2S_0$ conformation, and thus, some repulsion electrostatic energy is released since charges become further dispersed.

The use of the smaller possible model of heparin, a trisaccharide, has allowed us to determine that the behavior of the two types of glycosidic linkages, GlcN-IdoA and IdoA-GlcN, is not equivalent. We have detected weak NOE peaks corresponding to minor *anti*-Ψ rotameric populations in the case of the IdoA-GlcN linkage that were not observed for the GlcN-IdoA union. We propose that this is the flexibility point where the heparin chain can bend to form a kink, in order to adapt to the shape of the protein binding site.

Moreover, it is noticeable that, in the case described herein, the sulphation pattern significantly affects the "local" conformational properties (central ring) but not the "global" ones (determined by the Φ and Ψ torsions). This is one of the features that enhances heparin-like GAGs as biomolecules with a "special plasticity", which apparently play a key role in their bioactivities.

Owing to the asymmetry of the compounds some conclusions can be extracted about the factors that rule the conformational properties of the iduronate ring. Most of the previous data on this conformational equilibrium come from regularly substituted fragments of heparin, finding that in some cases the substitution of the neighbor ring affects clearly the iduronate conformational equilibrium.[34] We have found however an almost constant behavior with, at room temperature, a participation of the $^1C_4$ and $^2S_0$ in a 60–40 approximate ratio, nearly independently on the pattern of substituents of the ring at the reducing end terminus. From this observation it can be concluded that the modulation of the conformational properties of the iduronate by the adjacent rings comes mainly from the residue at the 4 position.

Another interesting observation was the increase of the correlation time caused by the presence of a sulfate group in position 6 of reducing end glucosamine. A feasible explanation is the increase on rigidity caused by charge repulsion in that part of the molecule.

Experimental Section

Synthesis: As an example we describe the synthesis of **Tri8**, the rest of the trisaccharides and the general procedures are described in the Supporting Information.

*Isopropyl O-(2-azido-3-O-benzyl-4,6-O-benzylidene-2-deoxy-α-D-glucopyranosyl)-(1→4)-O-(methyl 3-O-benzyl-2-O-pivaloyl-α-L-idopyranosyluronate)-(1→4)-2-acetamido-2-deoxy-3,6-di-O-benzyl-α-D-glucopyranoside (**10**)*: TMSOTf (3 μL, 0.017 mmol) was added to a solution of **1** (74 mg, 0.17 mmol) and **5** (177 mg, 0.198 mmol) in dry CH_2Cl_2 (4 mL), containing 4 Å molecular sieves and under argon atmosphere. After stirring for 30 min at RT, Et_3N (200 μL) was added and the solvent was evaporated. The residue was purified by flash chromatography (toluene/EtOAc = 4:1, 2:1, and 1:1) to yield **10** (175 mg, 75 %). $[\alpha]_D^{20} = +24.5°$ (c = 0.8, $CHCl_3$); TLC (toluene/EtOAc = 2:1) $R_f = 0.20$; ^{1}H NMR (500 MHz, $CDCl_3$): δ = 7.44–7.40 (m, 2H; PhH), 7.37–7.24 (m, 19H; PhH), 7.23–7.17 (m, 4H; PhH), 5.50 (s, 1H; $PhCHO_2$), 5.26 (d, $J_{1,2}$ = 4.0 Hz, 1H; H_{1b}), 5.22 (d, $J_{NH,2}$ = 9.5 Hz, 1H; CH_3CONH), 4.98 (t, $J_{2,1} = J_{2,3}$ = 4.0 Hz, 1H; H_{2b}), 4.93 (d, $J_{1,2}$ = 3.5 Hz, 1H; H_{1c}), 4.88 (d, J = 11.0 Hz, 1H; PhCH), 4.86 (d, $J_{1,2}$ = 4.0 Hz, 1H; H_{1a}), 4.78 (d, $J_{5,4}$ = 4.0 Hz, 1H; H_{5b}), 4.75 (AB-system, 2H; $PhCH_2$), 4.74 (d, J = 11.5 Hz, 1H; PhCH), 4.68 (d, J = 11.0 Hz, 1H; PhCH), 4.57 (ABsystem, 2H; $PhCH_2$), 4.50 (d, J = 11.5 Hz, 1H; PhCH), 4.25 (dd, $J_{6,5}$ = 5.5 Hz, $J_{6,6'}$ = 10.0 Hz, 1H; H_{6c}), 4.23 (td, $J_{2,1}$ = 3.5 Hz, $J_{NH,2} = J_{2,3}$ = 10.0 Hz, 1H; H_{2a}), 4.08 (t, $J_{4,3} = J_{4,5}$ = 9.0 Hz, 1H; H_{4a}), 4.03 (t, $J_{4,3} = J_{4,5}$ = 4.5 Hz, 1H; H_{4b}), 4.00 (t, $J_{3,2} = J_{3,4}$ = 4.5 Hz, 1H; H_{3b}), 3.93 (t, $J_{3,2} = J_{3,4}$ = 9.5 Hz, 1H; H_{3c}), 3.87 (td, $J_{5,6}$ = 5.5 Hz, $J_{5,4} = J_{5,6'}$ = 10.0 Hz, 1H; H_{5c}), 3.82 (hept, J = 6.5 Hz, 1H; CH *i*Pr), 3.81 (br d, $J_{6,6'}$ = 9.5 Hz, 1H; H_{6a}), 3.78 (m, 1H; H_{5a}), 3.66 (br d, $J_{6',6}$ = 9.5 Hz, 1H; $H_{6a'}$), 3.61 (br t, $J_{4,3} = J_{4,5} = J_{6',5} = J_{6',6}$ = 9.5 Hz, 2H; $H_{4c} + H_{6c'}$), 3.57 (t, $J_{3,2} = J_{3,4}$ = 10.0 Hz, 1H; H_{3a}), 3.42 (s, 3H; CH_3OCO), 3.31 (dd, $J_{2,1}$ = 4.0 Hz, $J_{2,3}$ = 9.5 Hz, 1H; H_{2c}), 1.75 (s, 3H; CH_3CONH), 1.16 (d, J = 6.5 Hz, 3H; CH_3 *i*Pr), 1.15 (s, 9H; CH_3 Piv), 1.07 ppm (d, J = 6.0 Hz, 3H; CH_3 *i*Pr); ^{13}C NMR (125 MHz, $CDCl_3$): δ = 177.59, 169.51, 169.13 (C=O), 138.63, 138.18, 137.73, 137.53, 137.34 (C Ph), 128.96, 128.39, 128.25, 128.18, 128.09, 127.85, 127.70, 127.59, 127.34, 127.25, 126.08 (CH Ph), 101.49 ($PhCHO_2$), 99.50 (C_{1c}), 97.80 (C_{1b}), 95.74 (C_{1a}), 82.47 (C_{4c}), 78.50 (C_{3a}), 76.06 (C_{3c}), 75.91 (C_{3b}), 75.20 (C_{4b}), 74.80 ($PhCH_2$), 74.68 (C_{4a}), 73.63, 73.28, 73.15 ($PhCH_2$), 71.08 (C_{5a}), 70.01 (CH *i*Pr), 69.81 (C_{2b}), 69.34 (C_{5b}), 68.47 (C_{6c}), 68.34 (C_{6a}), 63.22 (C_{5c}), 63.00 (C_{2c}), 52.12 (C_{2a}), 51.84 (CH_3OCO), 38.78 (C Piv), 27.15 (CH_3 Piv), 23.26 (CH_3CONH), 23.22, 21.57 ppm (CH_3 *i*Pr); HRMS: m/z calcd for $C_{64}H_{76}N_4O_{17}+Na^+$: 1195.5103 $[M+Na]^+$; found: 1195.5029.

*Isopropyl O-(2-azido-3-O-benzyl-4,6-O-benzylidene-2-deoxy-α-D-glucopyranosyl)-(1→4)-O-(3-O-benzyl-α-L-idopyranosyluronic acid)-(1→4)-2-acetamido-2-deoxy-3,6-di-O-benzyl-α-D-glucopyranoside (**14**)*: H_2O_2 (0.9 mL) and an aqueous LiOH solution (1.3 mL; 1 N) were added to a solution of **10** (70 mg, 0.060 mmol) in THF (3.1 mL) at 0 °C, 30 %. After stirring for 24 h at RT, the mixture was cooled at 0 °C, MeOH (4.8 mL) and an aqueous KOH solution (2.6 mL; 3 N) were added, and the mixture was stirred at 0 °C for 10 min. After stirring for 24 h at RT, the reaction mixture was acidified with IR-120-H^+ amberlite resin, filtered and concentrated. The residue was eluted from a Sephadex LH-20 chromatography column (MeOH/CH_2Cl_2 = 1:1) to afford 14 (56 mg, 87 %). $[\alpha]_D^{20} = +8.36°$ (c = 1.1, MeOH); TLC (CH_2Cl_2/MeOH = 25:1) $R_f = 0.15$; ^{1}H NMR (500 MHz, CD_3OD): δ = 7.51–7.45 (m, 5H; PhH), 7.42–7.21 (m, 20H; PhH), 5.61 (s, 1H; $PhCHO_2$), 5.22 (d, $J_{1,2}$ = 2.0 Hz, 1H; H_{1b}), 5.15 (d, $J_{1,2}$ = 4.0 Hz, 1H; H_{1c}), 5.00 (d, J = 11.5 Hz, 1H; PhCH), 4.95 (d, J =

11.5 Hz, 1H; PhCH), 4.85 (d, $J_{1,2}$=4.0 Hz, 1H; H_{1a}), 4.83 (brd, $J_{5,4}$= 2.0 Hz, 1H; H_{5b}), 4.78 (d, J=11.5 Hz, 1H; PhCH), 4.75 (s, 2H; $PhCH_2$), 4.60 (ABsystem, 2H; $PhCH_2$), 4.57 (d, J=12.0 Hz, 1H; PhCH), 4.40 (dd, $J_{6,5}$=5.0 Hz, $J_{6,6'}$=10.0 Hz, 1H; H_{6c}), 4.38 (brt, $J_{4,3}$=$J_{4,5}$=3.0 Hz, 1H; H_{4b}), 4.15 (td, $J_{5,6}$=5.5 Hz, $J_{5,4}$=$J_{5,6'}$=10.0 Hz, 1H; H_{5c}), 4.14 (t, $J_{3,2}$= $J_{3,4}$=9.5 Hz, 1H; H_{3c}), 4.10 (dd, $J_{2,1}$=3.5 Hz, $J_{2,3}$=10.5 Hz, 1H; H_{2a}), 3.95 (m, 1H; H_{3b}), 3.94 (m, 2H; H_{4a}+H_{5a}), 3.89 (m, 1H; H_{6a}), 3.88 (hept, J= 6.0 Hz, 1H; CH *i*Pr), 3.82 (m, 1H; H_{3a}), 3.81 (brt, $J_{2,1}$=$J_{2,3}$=3.0 Hz, 1H; H_{2b}), 3.731 (dd, $J_{2,1}$=4.0 Hz, $J_{2,3}$=10.0 Hz, 1H; H_{2c}), 3.728 (m, 1H; $H_{6a'}$), 3.72 (t, $J_{4,3}$=$J_{4,5}$=9.5 Hz, 1H; H_{4c}), 3.69 (t, $J_{6',5}$=$J_{6',6}$=10.0 Hz, 1H; $H_{6c'}$), 1.77 (s, 3H; CH_3CONH), 1.25 (d, J=6.0 Hz, 3H; CH_3 *i*Pr), 1.15 ppm (d, J=6.0 Hz, 3H; CH_3 *i*Pr); ^{13}C NMR (125 MHz, CD_3OD): δ=173.30, 173.18 (C=O), 140.15 (C Ph), 139.47 (3×C Ph), 139.05 (C Ph), 129.89, 129.40, 129.27, 129.18, 129.12, 129.08, 129.05, 129.02, 128.84, 128.72, 128.66, 128.41, 128.18, 127.25 (CH Ph), 103.56 (C_{1b}), 102.44 ($PhCHO_2$), 97.16 (C_{1c}), 96.87 (C_{1a}), 83.57 (C_{4c}), 80.67 (C_{3a}), 79.00 (C_{3c}), 78.67 (C_{3b}), 76.09 (C_{4a}), 75.87, 75.41 ($PhCH_2$), 74.79 (C_{4b}), 74.44, 73.18 ($PhCH_2$), 72.24 (C_{5a}), 71.34 (C_{5b}), 71.31 (CH *i*Pr), 70.09 (C_{6a}), 69.59 (C_{2b}+C_{6c}), 65.13 (C_{2c}), 64.22 (C_{5c}), 54.50 (C_{2a}), 23.67 (CH_3 *i*Pr), 22.60 (CH_3CONH), 21.61 ppm (CH_3 *i*Pr). MS (ESI) *m/z* positive mode: 1197.3 $[M+Na]^+$; *m/z* negative mode: 1073.4 $[M-H]^-$.

*Isopropyl O-(2-azido-3-O-benzyl-4,6-O-benzylidene-2-deoxy-α-*D*-glucopyranosyl)-(1→4)-O-(3-O-benzyl-2-O-sulfo-α-*L*-idopyranosyluronic acid)-(1→4)-2-acetamido-2-deoxy-3,6-di-O-benzyl-α-*D*-glucopyranoside triethylammonium salt (**18**)*: Sulfur trioxide-trimethylamine complex (46 mg, 0.33 mmol) was added to a solution of **14** (36 mg, 0.033 mmol) in dry DMF (3.3 mL). After stirring for 72 h at 50 °C under argon atmosphere, Et_3N (100 μL) was added and the solution stirred at RT for 5 min. The solution was purified by Sephadex LH-20 chromatography (MeOH/ CH_2Cl_2=1:1), and C-18 reverse phase chromatography (0% to 100% of MeOH in a 10 mM Et_3NHOAc aq. solution) to give 18 (35 mg, 78%). $[\alpha]_D^{20}$=+16.14° (*c*=1.4, MeOH); TLC (60/5/3/1 EtOAc/Py/H_2O/AcOH) R_f=0.30; ^{1}H NMR (500 MHz, CD_3OD): δ=7.53–7.46 (m, 6H; PhH), 7.41–7.23 (m, 16H; PhH), 7.21–7.17 (m, 3H; PhH), 5.62 (s, 1H; $PhCHO_2$), 5.44 (brs, 1H; H_{1b}), 5.12 (brs, 1H; H_{1c}), 4.96 (brs, 1H; H_{5b}), 4.95–4.87 (m, 3H; 3×PhCH), 4.84 (d, $J_{1,2}$=3.5 Hz, 1H; H_{1a}), 4.80 (d, J= 11.5 Hz, 1H; PhCH), 4.77 (d, J=11.5 Hz, 1H; PhCH), 4.73 (d, J= 11.0 Hz, 1H; PhCH), 4.67 (brs, 1H; H_{2b}), 4.60 (d, J=12.0 Hz, 1H; PhCH), 4.51 (d, J=12.5 Hz, 1H; PhCH), 4.31 (brd, $J_{6,6'}$=10.0 Hz, 1H; H_{6c}), 4.30 (brt, $J_{3,2}$=$J_{3,4}$=4.0 Hz, 1H; H_{3b}), 4.22 (brs, 1H; H_{4b}), 4.13 (brd, $J_{6,6'}$=11.0 Hz, 1H; H_{6a}), 4.08 (m, 1H; H_{2a}), 4.01 (m, 1H; H_{3c}), 4.00 (m, 1H; H_{5c}), 3.98 (t, $J_{4,3}$=$J_{4,5}$=9.5 Hz, 1H; H_{4a}), 3.94 (brd, $J_{5,4}$=10.0 Hz, 1H; H_{5a}), 3.89 (hept, J=6.0 Hz, 1H; CH *i*Pr), 3.76 (t, $J_{3,2}$=$J_{3,4}$=9.5 Hz, 1H; H_{3a}), 3.75 (brd, $J_{6',6}$=11.0 Hz, 1H; $H_{6a'}$), 3.73 (t, $J_{4,3}$=$J_{4,5}$=10.0 Hz, 1H; H_{4c}), 3.70 (brd, $J_{6',6}$=10.0 Hz, 1H; $H_{6c'}$), 3.53 (brd, $J_{2,3}$=10.0 Hz, 1H; H_{2c}), 2.99 (brq, J=7.0 Hz, 12H; CH_2 Et_3NH^+), 1.68 (s, 3H; CH_3CONH), 1.26 (d, J=6.5 Hz, 3H; CH_3 *i*Pr), 1.18 (brt, J=7.0 Hz, 18H; CH_3 Et_3NH^+), 1.16 ppm (d, J=6.0 Hz, 3H; CH_3 *i*Pr); ^{13}C NMR (125 MHz, CD_3OD): δ=174.91, 173.13 (C=O), 140.65, 140.02, 139.87, 139.62, 139.27 (C Ph), 129.74, 129.39, 129.33, 129.26, 129.11, 129.04, 128.95, 128.71, 128.62, 128.54, 128.35, 128.03, 127.16 (CH ì Ph), 102.18 ($PhCHO_2$), 100.61 (C_{1b}), 97.61 (C_{1c}), 96.97 (C_{1a}), 83.67 (C_{4c}), 80.64 (C_{3a}), 78.42 (C_{3c}), 76.64 (C_{4a}), 75.71, 75.42, 74.20 ($PhCH_2$), 73.28 (C_{3b}), 73.08 (C_{4b}), 73.02 ($PhCH_2$), 72.51 (C_{5a}), 72.04 (C_{2b}), 71.35 (CH *i*Pr), 69.83 (C_{6a}), 69.67 (C_{6c}), 69.13 (C_{5b}), 64.92 (C_{2c}), 64.21 (C_{5c}), 54.82 (C_{2a}), 47.41 (CH_2 Et_3NH^+), 23.65 (CH_3 *i*Pr), 22.46 (CH_3CONH), 21.66 (CH_3 *i*Pr), 9.16 (CH_3 Et_3NH^+); MS (ESI): *m/z* positive mode: 1215.4 $[M-2Et_3NH+Na+K+H]^+$, 619.2 $[M-2Et_3NH+2Na+K+H]^{2+}$; *m/z* negative mode: 1153.5 $[M-2Et_3NH+H]^-$.

*Isopropyl O-(3-O-benzyl-4,6-O-benzylidene-2-deoxy-2-sulfamido-α-*D*-glucopyranosyl)-(1→4)-O-(3-O-benzyl-2-O-sulfo-α-*L*-idopyranosyluronic acid)-(1→4)-2-acetamido-2-deoxy-3,6-di-O-benzyl-α-*D*-glucopyranoside sodium salt (**22**)*: An aqueous NaOH solution (1.9 mL; 0.1 N) and then a trimethylphosphine THF solution (184 μL; 1.0 M) were added dropwise to a solution of **18** (31 mg, 0.023 mmol) in THF (2.3 mL) at 0 °C and the mixture was stirred at RT. After 4 h, the solution was neutralized with an aqueous HCl solution (0.1 N), the solvents were evaporated until dryness and the resulting crude was suspended in MeOH, filtered, concentrated, and dried under high vacuum overnight (TLC (60/5/3/1 EtOAc/Py/H_2O/AcOH) R_f=0.61; MS (ESI): *m/z* positive mode: 1173.4 $[M+Na]^+$, 1151.4 $[M+H]^+$; *m/z* negative mode: 1149.4 $[M-H]^-$, 1127.4 $[M-Na]^-$). Triethylamine (0.5 mL) and sulfur trioxide-pyridine complex (19 mg, 0.12 mmol) were added to a solution of the crude in pyridine (2.5 mL), After stirring for 30 min at RT under argon atmosphere, the solution was purified by Sephadex LH-20 (MeOH/CH_2Cl_2=1:1), C-18 reverse phase chromatography (0% to 100% of MeOH in a 10 mM Et_3NHOAc aq. solution), again Sephadex LH-20 column (MeOH/CH_2Cl_2=1:1), and finally passed through a Dowex 50WX4-Na^+ column (MeOH/H_2O=9:1) to give **22** (24 mg, 82%). Characterization of **22** as triethylammonium salt: $[\alpha]_D^{20}$=+25.70° (*c*=1.0, MeOH); TLC (15/5/3/1 EtOAc/Py/H_2O/AcOH) R_f=0.30; ^{1}H NMR (500 MHz, CD_3OD): δ=7.52 (brt, J=7.5 Hz, 4H; PhH), 7.49 (brd, J=7.5 Hz, 2H; PhH), 7.44 (m, 2H; PhH), 7.38–7.16 (m, 14H; PhH), 7.18 (brt, J=7.5 Hz, 1H; PhH), 7.13 (brd, J=7.5 Hz, 2H; PhH), 5.58 (s, 1H; $PhCHO_2$), 5.57 (brs, 1H; H_{1b}), 5.48 (d, $J_{1,2}$=3.5 Hz, 1H; H_{1c}), 5.05 (d, J=12.5 Hz, 1H; PhCH), 4.96 (brs, 1H; H_{5b}), 4.94 (d, J=12.5 Hz, 1H; PhCH), 4.91 (d, J=12.0 Hz, 1H; PhCH), 4.84 (ABsystem, 2H; $PhCH_2$), 4.83 (d, $J_{1,2}$=3.5 Hz, 1H; H_{1a}), 4.78 (d, J=11.5 Hz, 1H; PhCH), 4.72 (brs, 1H; H_{2b}), 4.58 (d, J=11.5 Hz, 1H; PhCH), 4.52 (brs, 1H; H_{3b}), 4.46 (dd, $J_{6,5}$=5.0 Hz, $J_{6,6'}$=10.0 Hz, 1H; H_{6c}), 4.38 (d, J= 13.0 Hz, 1H; PhCH), 4.29 (brs, 1H; H_{4b}), 4.28 (brd, $J_{6,6'}$=11.0 Hz, 1H; H_{6a}), 4.10 (td, $J_{5,6}$=5.0 Hz, $J_{5,4}$=$J_{5,6'}$=10.0 Hz, 1H; H_{5c}), 3.95 (dd, $J_{2,1}$= 3.5 Hz, $J_{2,3}$=10.5 Hz, 1H; H_{2a}), 3.91 (m, 2H; H_{4a}+H_{5a}), 3.87 (hept, J= 6.0 Hz, 1H CH *i*Pr), 3.75 (t, $J_{3,2}$=$J_{3,4}$=9.5 Hz, 1H; H_{3c}), 3.71 (m, 2H; H_{3a}+$H_{6a'}$), 3.64 (t, $J_{6',6}$=$J_{6',5}$=10.5 Hz, 1H; $H_{6c'}$), 3.62 (t, $J_{4,3}$=$J_{4,5}$= 10.5 Hz, 1H; H_{4c}), 3.59 (dd, $J_{2,1}$=3.5 Hz, $J_{2,3}$=10.0 Hz, 1H; H_{2c}), 2.99 (q, J=7.5 Hz, 18H; CH_2 Et_3NH^+), 1.55 (s, 3H; CH_3CONH), 1.25 (d, J= 6.0 Hz, 3H; CH_3 *i*Pr), 1.20 (t, J=7.5 Hz, 27H; CH_3 Et_3NH^+), 1.13 ppm (d, J=6.0 Hz, 3H; CH_3 *i*Pr); ^{13}C NMR (100 MHz, CD_3OD): δ=176.17, 173.06 (C=O), 141.08, 140.94, 140.45, 140.24, 139.72 (C Ph), 129.50, 129.39, 129.28, 129.18, 129.10, 129.06, 129.03, 128.96, 128.91, 128.69, 128.53, 128.35, 128.09, 127.98, 127.12 (CH Ph), 102.35 (C_{1c}), 101.77 ($PhCHO_2$), 100.00 (C_{1b}), 96.90 (C_{1a}), 83.27 (C_{4c}), 80.84 (C_{3a}), 78.47 (C_{4b}), 78.25 (C_{3c}), 76.57 (C_{3b}+C_{4a}), 75.95, 75.60, 74.23, 73.02 ($PhCH_2$), 72.68 (C_{2b}+C_{5a}), 71.30 (CH *i*Pr), 69.97 (C_{6a}), 69.91 (C_{5b}), 69.85 (C_{6c}), 64.34 (C_{5c}), 60.78 (C_{2c}), 55.06 (C_{2a}), 47.41 (CH_2 Et_3NH^+), 23.64 (CH_3 *i*Pr), 22.45 (CH_3CONH), 21.65 (CH_3 *i*Pr), 9.42 ppm (CH_3 Et_3NH^+); MS (ESI): *m/z* positive mode: 1291.3 $[M-3Et_3NH+2Na+K+H]^+$, 1247.7 $[M-3Et_3NH+K+3H]^+$, 1231.8 $[M-3Et_3NH+Na+3H]^+$.

*Isopropyl O-(2-deoxy-2-sulfamido-α-*D*-glucopyranosyl)-(1→4)-O-(2-O-sulfo-α-*L*-idopyranosyluronic acid)-(1→4)-2-acetamido-2-deoxy-α-*D*-glucopyranoside sodium salt (**Tri8**)*: A solution of **22** (24 mg, 0.019 mmol) in a MeOH/H_2O=9:1 mixture (3.8 mL) was hydrogenated in the presence of 20% $Pd(OH)_2$/C. After 18 h, the suspension was filtered through a pad of celite and lyophilized to give **Tri8** (15 mg, 96%). $[\alpha]_D^{20}$=+66.0° (*c*=0.5, H_2O); TLC (5/5/3/1 EtOAc/Py/H_2O/AcOH) R_f=0.29; ^{1}H NMR (500 MHz, D_2O): δ=5.32 (d, $J_{1,2}$=3.5 Hz, 1H; H_{1c}), 5.15 (d, $J_{1,2}$=3.0 Hz, 1H; H_{1b}), 4.92 (d, $J_{1,2}$=3.5 Hz, 1H; H_{1a}), 4.69 (d, $J_{5,4}$=2.5 Hz, 1H; H_{5b}), 4.25 (dd, $J_{2,1}$=3.0 Hz, $J_{2,3}$=5.5 Hz, 1H; H_{2b}), 4.16 (dd, $J_{3,2}$=4.0 Hz, $J_{3,4}$= 5.5 Hz, 1H; H_{3b}), 4.03 (t, $J_{4,3}$=$J_{4,5}$=3.5 Hz, 1H; H_{4b}), 3.84 (hept, J= 6.0 Hz, 1H; CH *i*Pr), 3.83 (m, 3H, H_{5a}+H_{6a}+$H_{6a'}$), 3.82 (dd, $J_{2,1}$=4.0 Hz, $J_{2,3}$=9.5 Hz, 1H; H_{2a}), 3.80 (dd, $J_{6,5}$=2,0 Hz, $J_{6,6'}$=12.0 Hz, 1H; H_{6c}), 3.77 (m, 2H; H_{4a}+H_{5c}), 3.72 (dd, $J_{6',5}$=4.5 Hz, $J_{6',6}$=12.0 Hz, 1H; $H_{6c'}$), 3.65 (t, $J_{3,2}$=$J_{3,4}$=9.0 Hz, 1H; H_{3a}), 3.58 (dd, $J_{3,4}$=9.5 Hz, $J_{3,2}$=10.5 Hz, 1H; H_{3c}), 3.39 (t, $J_{4,3}$=$J_{4,5}$=9.5 Hz, 1H; H_{4c}), 3.15 (dd, $J_{2,1}$=3.5 Hz, $J_{2,3}$= 10.5 Hz, 1H; H_{2c}), 1.97 (s, 3H; CH_3CONH), 1.15 (d, J=6.0 Hz, 3H; CH_3 *i*Pr), 1.07 ppm (d, J=6.0 Hz, 3H; CH_3 *i*Pr); ^{13}C NMR (125 MHz, D_2O): δ=176.26, 175.75 (C=O), 100.63 (C_{1b}), 98.14 (C_{1c}), 96.25 (C_{1a}), 78.94 (C_{3a}), 77.20 (C_{2b}), 77.07 (C_{4b}), 73.09 (C_{5c}), 72.43 (C_{3c}), 72.27 (CH *i*Pr), 71.31 (C_{4c}), 70.91 (C_{4a}+C_{5a}), 70.36 (C_{5b}), 70.01 (C_{3b}), 61.68 (C_{6c}), 61.39 (C_{6a}), 59.44 (C_{2c}), 55.40 (C_{2a}), 23.65 (CH_3 *i*Pr), 23.19 (CH_3CONH), 21.86 ppm (CH_3 *i*Pr); MS (ESI): *m/z* positive mode: 849.1 $[M+Na]^+$, 843.1 $[M-Na+K+H]^+$; *m/z* negative mode: 803.1 $[M-Na]^-$, 797.1 $[M-3Na+K+H]^-$, 781.1 $[M-2Na+H]^-$, 390.0 $[M-2Na]^{2-}$.

NMR: NMR experiments were performed on Bruker DRX 500 MHz spectrometer equipped with 5 mm inverse triple-resonance probe. NMR samples were prepared at pH* ≃7 in 500–600 or 200 μL in 5 mm or 3 mm tubes, at 2 mM and 6 mM, respectively, in 99.9% D_2O and at several temperatures varying from 278 to 318 K. Sizes of acquisition matrices were

2 K×512 for COSY-dqf, gradient selected, experiments and 1 K×256 for TOCSY with mixing time of 80 ms. HSQC were recorded in gradient enhanced versions using echo-antiecho detection both with or without decoupling during acquisition. When it was required presaturation was applied by low power irradiation at water frequency.

The preliminary results of the NOESY were unsatisfactory because the molecules were close to the zero crossing point and give very weak peaks. ROESY sequences were also applied but the strong coupling of the protons of the L-IdoA2S residue biased the results. No better results were obtained using T-ROESY. Therefore, we recorded all the NOESY experiments at 278 K to increase the correlation time in order to obtain negative NOE peaks. Additionally, the use of lower temperatures allowed us to exploit the increase of the population of the lowest energy conformations. The build-up experiments were acquired with 1D sequence selected with gradients spin echo (dpfgse)[25] and two spin echoes flanked by bipolar gradients during the mixing time (200, 300, 400, 500, 600, 700, 800, 1000, 1300, 1500 ms).

Molecular dynamics: All the molecular dynamics simulations have been carried out on the Finis Terrae cluster belonging to the Centro de Supercomputación de Galicia (CESGA), Spain, taking advantage of the prioritized computing time we have been awarded (ICTS CESGA 2010 call).

In all cases, the starting geometries were generated from the available data deposited in the Protein Data Bank (pdb code 1 hpn) and modified accordingly. The topologies were built with PREP LINK EDIT PARM module of Amber 5.0, employing the residues and the set of partial charges published by Pérez et al.[35] (the latter developed under the context of the set of parameters for carbohydrates PIM[36]) and the force fields *parm91*[37] of Amber and *glycam 93*[38] together with the set of Altona parameters for sulfates.[39] Two independent starting geometries of each heparin-like trisaccharide structure were built, one with the L-IdoA2S residue in the chair $^1C_4$ conformation and one with the L-IdoA2S in the $^2S_0$ skew boat geometry. Each of these models was immersed in a 41 Å-sided cube with pre-equilibrated TIP3P water molecules.

To equilibrate the system we have followed a protocol consisting of 10 steps. Firstly, only the water molecules are minimized, and then heated to 300 K. After, the water box together with the sodium ions are minimized and then followed by a short MD simulation. At this point, the system is minimized in the four following steps with positional restraints imposed on the solute, decreasing the force constant step by step from 20 to 5 kcal mol^{-1}. Finally, a non-restraint minimization is carried out.

The production dynamics simulations have been accomplished at a constant temperature of 300 K (by applying the Berendsen coupling algorithm for the temperature scaling)[40] and constant pressure (1 bar). The Particle Mesh Ewald Method,[37,41] (to introduce long range electrostatic effects) and periodic boundary conditions have also been used. The SHAKE algorithm for hydrogen atoms, which allows using a 2 fs time step, was also employed. Finally, a 9 Å cutoff was applied for the Lennard-Jones interactions.

MD simulations have been performed with the sander module of Amber 6.0, with explicit treatment of the 10 12 hydrogen bond potential, in agreement with the parameters set for sulphates we used.[42] A total of 16 MD simulations of 20 ns each were obtained. The trajectory coordinates were saved each 0.5 ps.

The data processing of the 16 generated trajectories has been done with the *ptraj* module of Amber 9.0, except for the Cremer–Pople puckering coordinates, which have been calculated with the Carnal module of Amber 5.0.

The final theoretical $^3J_{HH}$ values were obtained as averages for each of the models (L-IdoA in $^1C_4$ or in $^2S_0$) according to Equation (1). Thus, to obtain the populations of conformers ($^1C_4$ and $^2S_0$) of the L-IdoA ring in each trisaccharide, we have performed an iterative fitting of theoretical and experimental *J*-coupling data [(Eq. (1)] (the $^4C_1$ conformation was disregarded as no experimental support was obtained for it, particularly the exclusive D-GlcN-L-IdoA2S H5′-H5 NOE was not observed).

$$^3J^{exptl}_{m(m+1)} = f_{(^1C_4)} \; <^3J^{MD}_{m(m+1)}(^1C_4)> \; + f_{(^2S_0)} \; <^3J^{MD}_{m(m+1)}(^2S_0) \qquad (1)$$

In this equation $f(^1C_4)$ and $f(^2S_0)$ are the molar fractions of each conformer, $<^3J^{HH}_{m(m+1)}(^1C_4)>$ are the averages from MD, and *m* is an index that runs from 1 to 4. Therefore, the experimental $^3J_{HH}$ coupling constants were considered as averages of the MD-derived $^3J_{HH}$ for each conformer weighted on the molar fraction of each one. As the theoretical values were averages from MD simulations, they implicitly reflected the fluctuations around canonical conformations, which must be considered for this flexible hexopyranose ring,[28] particularly to account for the pseudorotational conformational space in the case of the skew boat conformer ($^2S_0$).

Acknowledgements

We thank the CSIC (Grant No. 201180E021), the Spanish Ministry of Science and Innovation (Grant No. CTQ2009–07168), the Junta de Andalucía (Grant No. P07-FQM-02969, and "Incentivo a Proyecto Internacional") and the European Union (FEDER support and Marie Curie Reintegration Grant) for financial support. We acknowledge CESGA and MICINN for co-financing the prioritized computing time awarded (ICTS-2009–40). J.C.M. acknowledges financial support from CSIC. J.A. acknowledges financial support from the MICINN through the Ramón y Cajal program.

[1] a) B. Casu, U. Lindahl, *Adv. Carbohydr. Chem. Biochem.* **2001**, *57*, 159–206; b) B. Mulloy, R. J. Linhardt, *Curr. Opin. Struct. Biol.* **2001**, *11*, 623–628; c) I. Capila, R. J. Linhardt, *Angew. Chem. Int. Ed.* **2002**, *41*, 390; d) U. Lindahl, J. P. Li, *Int. Rev. Cell Mol. Biol.* **2009**, *276*, 105–159.

[2] J. Choay, M. Petitou, J. C. Lormeau, P. Sinay, B. Casu, G. Gatti, *Biochem. Biophys. Res. Commun.* **1983**, *116*, 492–499.

[3] a) A. Dementiev, M. Petitou, J. M. Herbert, P. G. W. Gettins, *Nat. Struct. Mol. Biol.* **2004**, *11*, 863–867; b) M. Hricovini, M. Guerrini, A. Bisio, G. Torri, M. Petitou, B. Casu, *Biochem. J.* **2001**, *359*, 265–272; c) C. Laguri, N. Sapay, J. P. Simorre, B. Brutscher, A. Imberty, P. Gans, H. Lortat-Jacob, *J. Am. Chem. Soc.* **2011**, *133*, 9642–9645.

[4] a) H. E. Conrad, *Heparin Binding Proteins*, Academic Press, San Diego, **1988**; b) J. D. Esko, S. B. Selleck, *Annu. Rev. Biochem.* **2002**, *71*, 435–471.

[5] J. R. Bishop, M. Schuksz, J. D. Esko, *Nature* **2007**, *446*, 1030–1037.

[6] a) R. Raman, S. Raguram, G. Venkataraman, J. C. Paulson, R. Sasisekharan, *Nat. Methods* **2005**, *2*, 817–824; b) R. Raman, V. Sasisekharan, R. Sasisekharan, *Chem. Biol.* **2005**, *12*, 267–277; c) S. Khan, J. Gor, B. Mulloy, S. J. Perkins, *J. Mol. Biol.* **2010**, *395*, 504–521; d) S. Khan, E. Rodriguez, R. Patel, J. Gor, B. Mulloy, S. J. Perkins, *J. Biol. Chem.* **2011**, *286*, 24842–24854.

[7] B. Mulloy, M. J. Forster, C. Jones, D. B. Davies, *Biochem. J.* **1993**, *293*, 849–858.

[8] B. Mulloy, M. J. Forster, *Glycobiology* **2000**, *10*, 1147–1156.

[9] J. Angulo, R. Ojeda, J. L. de Paz, R. Lucas, P. M. Nieto, R. M. Lozano, M. Redondo-Horcajo, G. Gimenez-Gallego, M. Martin-Lomas, *ChemBioChem* **2004**, *5*, 55–61.

[10] a) M. J. Forster, B. Mulloy, *Biopolymers* **1993**, *33*, 575–588; b) S. Ernst, G. Venkataraman, V. Sasisekharan, R. Langer, C. L. Cooney, R. Sasisekharan, *J. Am. Chem. Soc.* **1998**, *120*, 2099–2107.

[11] L. Pellegrini, *Curr. Opin. Struct. Biol.* **2001**, *11*, 629–634.

[12] M. Guerrini, T. Agulles, A. Bisio, M. Hricovini, L. Lay, A. Naggi, L. Poletti, L. Sturiale, G. Torri, B. Casu, *Biochem. Biophys. Res. Commun.* **2002**, *292*, 222–230.

[13] J. L. de Paz, J. Angulo, J. M. Lassaletta, P. M. Nieto, M. Redondo-Horcajo, R. M. Lozano, G. Gimenez-Gallego, M. Martin-Lomas, *ChemBioChem* **2001**, *2*, 673–685.

[14] P. J. Garegg, H. Hultberg, S. Wallin, *Carbohydr. Res.* **1982**, *108*, 97–101.

[15] J. L. de Paz, R. Ojeda, N. Reichardt, M. Martin-Lomas, *Eur. J. Org. Chem.* **2003**, 3308–3324.
[16] J. L. de Paz, M. Martin-Lomas, *Eur. J. Org. Chem.* **2005**, 1849–1858.
[17] H. Lucas, J. E. M. Basten, T. G. Vandinther, D. G. Meuleman, S. F. Vanaelst, C. A. A. Vanboeckel, *Tetrahedron* **1990**, *46*, 8207–8228.
[18] a) S. Maza, G. Macchione, R. Ojeda, J. Lopez-Prados, J. Angulo, J. L. de Paz, P. M. Nieto, *Org. Biomol. Chem.* **2012**, *10*, 2146–2163; b) C. Noti, J. L. de Paz, L. Polito, P. H. Seeberger, *Chem. Eur. J.* **2006**, *12*, 8664–8686.
[19] A. Dilhas, R. Lucas, L. Loureiro-Morais, Y. Hersant, D. Bonnaffe, *J. Comb. Chem.* **2008**, *10*, 166–169.
[20] M. Sakagami, H. Hamana, *Tetrahedron Lett.* **2000**, *41*, 5547–5551.
[21] S. Maza, J. L. de Paz, P. M. Nieto, *Tetrahedron Lett.* **2011**, *52*, 441–443.
[22] Y.-P. Hu, S.-Y. Lin, C.-Y. Huang, M. M. L. Zulueta, J.-Y. Liu, W. Chang, S.-C. Hung, *Nat. Chem.* **2011**, *3*, 557–563.
[23] E. A. Yates, F. Santini, M. Guerrini, A. Naggi, G. Torri, B. Casu, *Carbohydr. Res.* **1996**, *294*, 15–27.
[24] S. Macura, B. T. Farmer, L. R. Brown, *J. Magn. Reson.* **1986**, *70*, 493–499.
[25] K. Stott, J. Keeler, Q. N. Van, A. J. Shaka, *J. Magn. Reson.* **1997**, *125*, 302–324.
[26] H. Hu, *J. Magn. Reson.* **2006**, *182*, 173–177.
[27] S. Macura, R. R. Ernst, *Mol. Phys.* **1980**, *41*, 95–117.
[28] J. Angulo, P. M. Nieto, M. Martin-Lomas, *Chem. Commun.* **2003**, 1512–1513.
[29] D. R. Ferro, A. Provasoli, M. Ragazzi, B. Casu, G. Torri, V. Bossennec, B. Perly, P. Sinay, M. Petitou, J. Choay, *Carbohydr. Res.* **1990**, *195*, 157–167.
[30] G. Lipari, A. Szabo, *J. Am. Chem. Soc.* **1982**, *104*, 4546–4559.
[31] M. Hricovíni, G. Torri, *Carbohydr. Res.* **1995**, *268*, 159–175.
[32] a) R. Ojeda, J. Angulo, P. M. Nieto, M. Martin-Lomas, *Can. J. Chem.* **2002**, *80*, 917–936; b) R. Lucas, J. Angulo, P. M. Nieto, M. Martin-Lomas, *Org. Biomol. Chem.* **2003**, *1*, 2253–2266.
[33] a) B. Casu, J. Choay, D. R. Ferro, G. Gatti, J. C. Jacquinet, M. Petitou, A. Provasoli, M. Ragazzi, P. Sinay, G. Torri, *Nature* **1986**, *322*, 215–216; b) D. R. Ferro, A. Provasoli, M. Ragazzi, G. Torri, B. Casu, G. Gatti, J. C. Jacquinet, P. Sinay, M. Petitou, J. Choay, *J. Am. Chem. Soc.* **1986**, *108*, 6773–6778; c) M. Ragazzi, D. R. Ferro, B. Perly, G. Torri, B. Casu, P. Sinay, M. Petitou, J. Choay, *Carbohydr. Res.* **1987**, *165*, c1–c5.
[34] B. Mulloy, M. J. Forster, C. Jones, A. F. Drake, A. E. A. Johnson, B. D. B. Davies, *Carbohydr. Res.* **1994**, *255*, 1–26.
[35] S. Pérez, C. Meyer, A. Imberty, *Mol. Eng.* **1995**, *5*, 271–300
[36] M. Clark, R. D. Cramer, N. Vanopdenbosch, *J. Comput. Chem.* **1989**, *10*, 982–1012.
[37] D. M. York, T. A. Darden, L. G. Pedersen, *J. Chem. Phys.* **1993**, *99*, 8345–8348.
[38] R. J. Woods, R. A. Dwek, C. J. Edge, B. Fraser-Reid, *J. Phys. Chem.* **1995**, *99*, 3832–3846.
[39] C. J. M. Huige, C. Altona, *J. Comput. Chem.* **1995**, *16*, 56–79.
[40] H. J. C. Berendsen, J. P. M. Postma, W. F. Vangunsteren, A. Dinola, J. R. Haak, *J. Chem. Phys.* **1984**, *81*, 3684–3690.
[41] H. G. Petersen, *J. Chem. Phys.* **1995**, *103*, 3668–3679.
[42] C. A. G. Haasnoot, F. A. A. M. de Leeuw, C. Altona, *Tetrahedron* **1980**, *36*, 2783–2792.

Received: August 1, 2012
Published online: November 9, 2012

